Synergistic Uptake by Acidic Sulfate Particles of Gaseous Mixtures of Glyoxal and Pinanediol

Yiming Qin (1), Jianhuai Ye (1), Paul E. Ohno (1,2), Yali Lei (1), Junfeng Wang (1), Pengfei Liu (1), Regan J. Thomson (3), and Scot T. Martin* (1,4)

- School of Engineering and Applied Sciences, Harvard University, Cambridge, Massachusetts, USA
- (2) Harvard University Center for the Environment, Harvard University, Cambridge,
 Massachusetts, USA
- (3) Department of Chemistry, Northwestern University, Evanston, Illinois, USA
- (4) Department of Earth and Planetary Sciences, Harvard University, Cambridge, Massachusetts, USA

E-mail: scot_martin@harvard.edu, ORCiD: 0000-0002-8996-7554

http://martin.seas.harvard.edu

Revision: July 2020

Environmental Science & Technology

*To Whom Correspondence Should be Addressed

Abstract

1

2

3

4

5

6

7

8

9

10

11

12

13

14

15

16

The uptake of gaseous organic species by atmospheric particles can be affected by the reactive interactions among multiple co-condensing species, yet the underlying mechanisms remain poorly understand. Here, the uptake of unary and binary mixtures of glyoxal and pinanediol by neutral and acidic sulfate particles is investigated. These species are important products from the oxidation of volatile organic compounds (VOCs) under atmospheric conditions. The uptake to acidic aerosol particles greatly increased for a binary mixture of glyoxal and pinanediol compared to the unary counterparts. The strength of the synergism depended on the particle acidity and water content (i.e., relative humidity). The greater uptake was up to 2.5× to 8× at 10% RH for glyoxal and pinanediol, respectively. At 50% RH, it was 2× and 1.2× for the two species. Possible mechanisms of acid-catalyzed cross reactions between the species are proposed to explain the synergistic uptake. The proposed mechanisms are applicable to a broader extent across atmospheric species having carbonyl and hydroxyl functionalities. The results thus suggest that synergistic uptake reactions can be expected to significantly influence the gas-particle partitioning of VOC oxidation products under atmospheric conditions and thus greatly affect their atmospheric transport and lifetime.

1. Introduction

Atmospheric particles play significant roles in climate, air quality, and human health. ^{1–3}
Particles can be formed through in situ nucleation of gas vapors in the atmosphere or directly emitted to the atmosphere from sources. ^{4,5} Once particles are formed, condensational growth from gas vapors in the atmosphere can take place, and additional chemistry can occur inside the particles, leading to the depletion of gas-phase species and thereby providing a thermodynamic driving force for the deposition of additional reactants from the gas phase, further growing the particles. ^{6–8} This uptake of gas-phase species into the particle phase and the subsequent particle-phase chemical reactions not only affect the mass concentration of organic particulate matter but also can greatly alter important physical properties of atmospheric particles, such as size, optical properties, and surface tension. ^{9–11} Despite the importance of particle-phase chemical reactions to these properties, a comprehensive understanding of these processes is still lacking due to the chemical complexity of the gas-phase molecules and the numerous possible reactions that could occur in the particle phase. ^{12,13}

The uptake of a gaseous organic species by particles can be described by an uptake coefficient that incorporates processes including gas-phase diffusion, surface mass accommodation, interfacial mass transport, and particle-phase diffusion and reactions. ^{14–16} Interactions between the original gas-phase species and the species in the particles, such as inparticle chemical reactions, can further shift partitioning and uptake from the gas to the particle phase, thereby leading to enhanced uptake. ^{17,18} Laboratory studies, focusing on the uptake of one single species such as ozone, ammonia, and organic compounds (e.g., glyoxal, pinonaldehyde, levoglucosan, and dicarboxylic acid), have provided a fundamental understanding on the uptake of gas species by particles. ^{19–28} However, atmospheric uptake usually occurs in the presence of

hundreds of organic species, rather than just a single compound. These accumulated species, which are relatively isolated from one another in the gas phase, become concentrated in the particle phase. They may thereby undergo chemical reactions in the particle phase that would be much slower in the gas phase. Whether and how the molecular and reactive interactions among multiple co-existing organic compounds affect gas-particle partitioning and uptake processes remain unclear.

40

41

42

43

44

45

46

47

48

49

50

51

52

53

54

55

56

57

58

59

60

61

62

The study herein focuses on the uptake of unary and binary mixtures of glyoxal and pinanediol by neutral and acidic sulfate particles. These species are important products from the oxidation of volatile organic compounds (VOCs) under atmospheric conditions. The global production of glyoxal as a C₂ product from the atmospheric oxidation of longer-chain VOCs, such as isoprene, other biogenic precursors, and anthropogenic species, is high (e.g., estimated as 45 Tg vr⁻¹).²⁹ Structurally, glyoxal is a dicarbonyl compound with the possibility to facilely hydrate in the presence of water and become a tetra-hydroxyl compound. For these reasons of occurrence and reactivity, glyoxal can be regarded as one of a handful of uniquely important atmospheric molecules in respect to gas-particle uptake.^{29–32} A key question is if its uptake can be further enhanced by possible synergistic reactions with the plethora of other atmospheric gaseous organic species that are abundant in type yet each individually of lower concentration than glyoxal. Pinanediol, a prominent oxidation product of α -pinene, is taken in this study as a prototypical example that may substantially enhance glyoxal uptake and thus overall production of organic particulate matter. More specifically, this model system of glyoxal and pinanediol is explored herein as broadly representative of possible synergisms in the uptake processes to atmospheric particles over tropical or boreal forests under the influence of upwind anthropogenic emissions that contribute to atmospheric concentrations of sulfate particles.

2. Experimental

The experimental setup consisted of four major components (Figure 1): particle generation, organic reactant volatilization, chamber for the reactive uptake, and particle-phase analytical measurements.

2.1 Particle Generation

Inorganic particles were aerosolized by a Model 3076 constant output atomizer (TSI Inc., Shoreview, MN). A solution of ammonium bisulfate (Sigma-Aldrich, >99.5% purity; 0.1 g L⁻¹) was atomized for the experiments that used acidic particles. A solution of ammonium sulfate (Sigma-Aldrich, >99.0% purity; 0.1 g L⁻¹) was used for the experiments that employed neutral particles.

2.2 Volatilization of Organic Reactants

Gas-phase reactants of glyoxal, pinanediol, and the binary mixture of glyoxal and pinanediol were produced by a syringe-nebulizer-evaporation system. An aqueous solution containing the reactants was pushed through a nebulizer (Meinhard A3, PerkinElmer Inc., Waltham, MA) by a syringe pump (Fusion 200, Chemyx Inc., Stafford, TX; liquid flow rate of 85.80 μL h⁻¹) at a pure-air flow rate of 0.7 L min⁻¹. The nebulized molecules were further diluted by a flow of zero air (4.3 L min⁻¹), thereby accelerating evaporation into the gas phase. For the experiments that employed only glyoxal as the gas-phase reactant molecule an aqueous solution of glyoxal, prepared as 2 g L⁻¹ from a 40 wt% commercial solution (Sigma-Aldrich), was nebulized. Glyoxal was below its aqueous solubility of 100 g L⁻¹ (NTP 1992). The prepared concentration was also below the polymerization threshold.^{33,34} For experiments that used only pinanediol as the gas-phase reactant molecule an aqueous solution of (-)-pinanediol, prepared as 2 g L⁻¹ from commercial crystals (≥99.0% purity, Sigma-Aldrich), was nebulized and

evaporated in the system. Pinanediol, for which no reliable solubility value could be found, was observed to fully solubilize in the prepared solution. In the case of the experiments that employed binary mixtures of glyoxal and pinanediol, an aqueous solution of glyoxal and pinanediol was used (2 g L⁻¹ of each). The gas-phase concentrations of the individual species of the binary mixture were thus the same as their unary counterparts.

After nebulization, the gas-phase concentrations of glyoxal and pinanediol were not directly measured. Instead, the gas-phase concentration of these species inside the reactor (section 2.3) was estimated based on mass balance with the nebulized solution and subsequent gas-phase dilution. The calculated pinanediol concentration was 20 ppb, which was lower than its gas-phase saturation concentration (293 ppb). Similarly, the calculated glyoxal concentration was 58 ppb, which was also below its gas-phase saturation concentration of 4.3×10^7 ppb. There should thus be no new particle formation within the apparatus. Glyoxal can undergo wall loss in the apparatus,³⁵ and the calculated concentrations are thus upper limits (Table S1).

2.3 Reactive Uptake Chamber

After the gas-phase species were nebulized and the particles were aerosolized, the individual flows were mixed. The gas flow of 0.78 L min⁻¹ and the particle flow of 2.42 L min⁻¹ were combined in a continuously mixed flow reactor (CMFR), in which uptake occurred. The reactor, which was a 22-L round-bottom glass flask, was placed in a temperature-controlled room at 20 °C. The residence time inside the CMFR was 390 s. The sampling line from the CMFR to the analytical instrumentation was Teflon tubing (outer diameter of 6.35 mm, length of 1 m). The estimated transit time through the tubing was 0.5 s. Relative humidity (RH) and temperature inside the CMFR were monitored by a Rotronic Sensor (Bassersdorf, Switzerland). The RH was controlled by a custom-built feedback control Nafion dry-wet air exchange system.

In individual experiments, the uptake of the gas-phase organic molecules by the initially organic-free sulfate particles was conducted for 3 to 12 h. After 2 h of spin up, quantities measured by all instrumentation became stable. The results presented herein were analyzed for the steady-state conditions of each experiment. When changing among the experiments, the chamber was flushed with zero air for 2 days.

2.4 Analytical Instrumentation

The outflow of the CMFR passed through the sampling lines to analytical instrumentation. The number-diameter distribution of the particle population was measured by a Scanning Mobility Particle Sizer (SMPS; Model 3080, TSI Inc., Shoreview, MN). The mode diameter of the aerosolized particle population was 60 to 70 nm, and uptake of the organic molecules did not significantly change the particle diameters (Figure S1). The chemical composition of the aerosol particles was analyzed with an Aerodyne Aerosol Mass Spectrometer (HR-ToF-AMS, Aerodyne Research Inc., Billerica, MA). The ratio of the mass concentration of organic tracer ions to that of inorganic species remained <2% for all uptake experiments (Tables S2 and S3). The AMS data analysis was performed in *Igor Pro* (WaveMetrics Inc., Lake Oswego, OR) using the Aerodyne *SQUIRREL* (v1.56D) and *PIKA* (v1.15D) toolkits. The ionization efficiency of the AMS was calibrated using particles of ammonium nitrate (Sigma-Aldrich, $\ge99.0\%$ purity). Mass concentrations were based on relative ionization efficiencies of 1.4 and 1.2 for organic and sulfate species, respectively, and a collection efficiency of unity.

3. Results

Figure 2 shows an example of the time series of tracer ions for glyoxal and pinanediol during an uptake experiment for both acidic and neutralized sulfate particles. The time series is divided into three panels with respect to exposure to gas-phase species. A detailed description for

the identification of tracer ions is presented in the Supplemental Information (Text S1). In brief, the tracer ions were identified by comparing the particle-phase signal intensities in the experiments with and without the exposure of the gas-phase organic species. For the unary uptake of glyoxal by ammonium bisulfate particles, there was a large increase in the signal intensity at m/z 58 ($C_2H_2O_2^+$) as compared to the blank condition (Figure S2). The same tracer ion has been previously used in the literature to track glyoxal uptake.³⁷ For the unary uptake of pinanediol by ammonium bisulfate particles, a peak was observed at m/z 91, while no contribution at m/z 58 was observed. No contribution at m/z 91 was observed for these glyoxal-only experiments. Therefore, the signal intensity of the $C_2H_2O_2^+$ ion traces the uptake of glyoxal while the signal intensity of the $C_3H_7O^+$ ion traces the uptake of pinanediol.

For Figure 2I-a, gas-phase glyoxal was added into the CMFR in the presence of the ammonium bisulfate particles. During this period, the average mass concentration of the $C_2H_2O_2^+$ ion (glyoxal tracer, shown in green) was $0.11\pm0.02~\mu g~m^{-3}$ whereas the average mass concentration of the $C_3H_7O^+$ ion (pinanediol tracer, blue) was $0.006\pm0.002~\mu g~m^{-3}$. The latter is close to the background level. For Figure 2I-b, there was no exposure to glyoxal and only exposure to gas-phase pinanediol. The average mass concentration of the $C_2H_2O_2^+$ ion decreased to the background level (< $0.01~\mu g~m^{-3}$) whereas the average mass concentration of the $C_3H_7O^+$ ion increased to $0.03\pm0.02~\mu g~m^{-3}$.

For Figure 2I-c, there was a binary mixture of glyoxal and pinanediol in the gas phase at similar concentrations to the unary exposures (Table S1). In the particle phase, the average mass concentration of the $C_2H_2O_2^+$ ion increased to $0.39 \pm 0.03 \,\mu g \, m^{-3}$, which was up to $4\times$ higher than in the experiments with glyoxal alone (panel *a*). The average mass concentration of the $C_3H_7O^+$ ion increased to $0.07 \pm 0.03 \,\mu g \, m^{-3}$, which was up to $3\times$ higher than in the experiments

with pinanediol alone (panel *b*). These results thus show that the uptake was much greater for both glyoxal and pinanediol in the case of a binary mixture compared to the unary counterparts. This conclusion holds for acidic ammonium bisulfate particles. In contradistinction, there was no synergistic effect for similar experiments that employed neutral ammonium sulfate particles (Figure 2II-a,b,c) (Table S2), thus highlighting the importance of acidity in modulating the amount of uptake of gas-phase organic molecules.

The possible role of wall loss in the interpretation of the experimental results can be considered. In CMFR operation, species concentrations on walls can saturate, and further wall loss can diminish. Even so, glyoxal and pinanediol may have different affinities for the walls,³⁵ as reflected in Figure 2 that the characteristic time required to reach steady state differs for the pinanediol and glyoxal tracers. Regardless of the extent of possible wall loss, however, the concentrations of glyoxal and pinanediol are expected to have the same value at steady state in both the unary and binary experiments because the same protocols were used regarding species generation and transport in the two sets of experiments, implying an equal extent of wall loss. The scientific interpretation herein is based on relative changes, so differences in wall loss and differences between actual concentrations and upper-limit concentrations (Table S1) do not complicate the scientific interpretation of the experiments. Wall loss does not affect the relative comparison of glyoxal uptake between the unary and binary experiments.

Relative humidity (RH) has been reported to affect the uptake of gas-phase organic species through modulation of the acidity and ionic strength of the aqueous phase of particles.^{24,25,30,38–41} The effect or not of RH on synergistic uptake was therefore examined in the present study. Particle-phase water and pH were estimated using *Extended AIM Aerosol*

Thermodynamics Model II (Table S2 and Table S3).⁴² Concentrations of the inorganic species and the organic tracer ions in the particle phase are also listed Table S3.

Figure 3a shows the concentration of the glyoxal C₂H₂O₂⁺ tracer ion as a function of RH. In this set of experiments, ammonium bisulfate particles were exposed to no organic gas-phase species (i.e., blank, shown in black), glyoxal alone (orange), or a binary mixture of glyoxal and pinanediol (green). For the blank experiments, across the studied range of 10% to 50% RH the mass concentrations of the glyoxal tracer ion remained within background (Figure 3a). Upon exposure to gas-phase glyoxal (orange), the mass concentrations of the glyoxal tracer ion increased several fold, but this relative increase had no trend as a function of RH in the unary exposure (Table S3). There is some evidence in the literature supporting the observation of minimal effect of RH on glyoxal uptake,³⁸ although previous reports on the role of RH and acidity on the magnitude of glyoxal uptake to particles did not conclusively determine the mechanism of uptake and in some cases reported conflicting results.^{24,30}

For the uptake of the binary mixture of glyoxal and pinanediol (green; Figure 3a), the average mass concentrations of the glyoxal tracer ion were greater than in the unary system for all RH (Table S3). The relative synergistic uptake of glyoxal, meaning the uptake in the binary compared to the unary experiments, was greater for the lower RH. More specifically, the increase in uptake increased from 2× at 50% RH to 2.5× at 10% RH. This trend with decreasing RH can be attributed to an associated decrease in the particle liquid water content (Table S3) and hence a stronger ionic strength as well as lower pH inside the particles. In other laboratory experiments, Jang et al.⁴³ also observed a decrease in the uptake of gas-phase glyoxal by acidic particles at higher RH when 1-decanol was added to the gas phase. In the ambient environment

Shen et al.⁴⁴ reported lower partitioning of glyoxal towards the particle phase at higher RH, possibly because of the co-existence of many hydroxyl-containing species.

For comparison to glyoxal, Figure 3b shows the mass concentration of the pinanediol C₃H₇O₃⁺ tracer ion as a function of RH. In this set of experiments, ammonium bisulfate particles were exposed to no organic gas-phase species (i.e., blank, shown in black), pinanediol alone (orange), or a binary mixture of glyoxal and pinanediol (green). The blank experiments confirmed that RH did not appreciably affect the background level of the pinanediol tracer ion. Upon exposure to unary gas-phase pinanediol (blue), the mass concentrations of the pinanediol tracer ion increased at higher RH (Table S3). This result differs from the result for glyoxal alone, for which the mass concentration of the glyoxal tracer ion remained unchanged for increasing RH (Figure 3a). The acid-catalyzed esterification of the pinanediol alcohol groups is expected to be slow,⁴⁵ decreasing the relative importance of chemical reactions to the amount of observed uptake for the case of unary pinanediol exposure. The increase in pinanediol uptake might occur because of the increase of particle liquid water content at higher RH and the water solubility of pinanediol.⁴⁶

In the experiments that used the binary mixture of glyoxal and pinanediol (green; Figure 3b), the average mass concentrations of the pinanediol tracer ion were greater in the binary mixture than in the unary system for all RH values, ranging from around 8× at 10% RH to 1.2× at 50% RH (Table S3). The relative synergistic uptake of pinanediol decreased by 6.8× from 10% RH to 50% RH, as was likewise observed for glyoxal (Figure 3a). A further noteworthy observation is that the relative uptake trend of pinanediol with RH shifted, meaning an increasing trend for pinanediol alone compared to a decreasing trend for the binary mixture.

4. Discussion

221

222

223

224

225

226

227

228

229

230

231

232

233

234

235

236

237

238

239

240

241

242

molecular weight can result.

The synergistic results presented in the two panels of Figure 3 demonstrate an important role for organic-organic interactions in the uptake of glyoxal and by extension highlight the possibility of similar processes under atmospheric conditions. In this regard, organic chemical reactions can be an intricate series of sequential and parallel steps that depend on a range of reactions conditions. For glyoxal uptake by neutral to alkaline ammonium sulfate particles, glyoxal and ammonia reactions can take place to produce hydrated N-glyoxal substituted imidazole and hydrated imidazole-2-carboxaldehyde (Figure 4, pathway a). 47-49 For acidic ammonium bisulfate particles, aqueous glyoxal can lead to the formation geminal diols (pathways b and c). This reaction can be followed further by hemiacetal/acetal polymer formation (pathway b) or glyoxal sulfate formation (pathway c). 23,51 The results presented herein showed synergism in the binary uptake of glyoxal and pinanediol by acidic sulfate particles. Understanding, quantifying, and modeling these synergistic organic-organic interactions can be complex. Corrigan et al.⁵² observed the crossreaction between glyoxal and alcohols for mildly acidic particles. Drozd et al.⁵³ likewise reported interactions between alcohols and glyoxal in the acidic sulfate solutions. For the synergistic uptake observed herein, Figure 4 illustrates several possible reaction pathways d, e, and f involving the formation of hemiacetal and acetal intermediates that can contribute to the observed synergism. In these pathways, glyoxal can undergo an initial acid-catalyzed condensation reaction to produce an intermediate hemiacetal, and this species in turn can follow

several different possible reaction pathways (e.g., pathways d, e, and f). Products of high

The relative importance of each pathway in Figure 4 is dependent upon factors such as the pH, temperature, and the relative ratios of glyoxal and pinanediol. At high concentrations of pinanediol, pathway d is favored. One molecule of glyoxal reacts with two or more molecules of pinanediol. Oligomeric acetal species of moderate molecular weight are produced. In some cases, these compounds may be stable, such as the bisacetal and the complex-adduct species. At high concentrations of glyoxal, pathway e is favored. Oligomers of high molecular weight and polymers of glyoxal can incorporate small amounts of pinanediol. When the concentrations of glyoxal and pinanediol are similar, linear co-polymers can be generated by pathway f.

The AMS mass spectra for m/z > 100 supports the foregoing interpretation. Higher intensities for ions of m/z > 100 are regarded in the AMS literature as general evidence for the presence of high-molecular-weight products in the sampled aerosol particles, as reported in Liggio et al.,²⁵ De Haan et al.,⁵⁴ Faust et al.,⁵⁵ and Riva et al.⁵⁶ The reason for this interpretation is that the AMS has an aggressive ionization scheme (i.e., 70 eV electron impact; EI) so that the detection of large fragments implies oligomeric or larger parent species. The AMS spectra can be compared for the uptake of (i) unary glyoxal, (ii) unary pinanediol, and (iii) binary glyoxal and pinanediol (Figure 5). There is a larger fraction of high-molecular-weight products for the binary case compared to either unary counterpart. This result supports the possibility that pathways like d, e, and f are active in the observed synergistic uptake. In the future, ultraviolet absorbance spectroscopy, electrospray-ionization mass spectrometry, nuclear magnetic resonance spectroscopy, and other complementary techniques can be recommended for gaining further information on the specific mechanisms and species responsible for the uptake synergism.

The observed uptake in these laboratory experiments might represent a lower limit of the total synergistic potential under atmospheric conditions. The exposure times in the experiments

are significantly shorter than particle atmospheric residence time. The implication could be that a kinetic limitation on uptake prevails for the laboratory experiments whereas a thermodynamic regime of total potential uptake might be active for the longer timescales of atmospheric processes. The dominant regime of a kinetic or thermodynamic limitation for uptake of a gaseous species to a particle can be considered within the framework of resistor model. 16,32,57. Within that framework, the diffusion of a molecule in the gas phase to the gas-particle interface, accommodation of the molecule into the particle surface region, possible chemical reactions within the surface region, and diffusion of the molecule from the surface region to the interior region of the particle do not appear to be rate-limiting in the present experiments (Section S2). Aqueous-phase chemical reactions, however, may occur more slowly than the CMFR residence time, implying in this case that the observed uptake could be in a kinetic regime. Similar (i.e., thermodynamic regime) or greater uptake (i.e., kinetic regime) compared to the laboratory experiments is thus expected for the longer interaction times of atmospheric processes.

These results highlight that the uptake of the numerous different organic species to particulate matter in the atmosphere cannot in many cases be accurately treated as independent processes of each species but rather must instead consider synergistic interactions among the species. The results presented herein show that the uptake of a binary mixture of glyoxal and pinanediol to acidic aerosol particles is greater than that of their unary counterparts. The greater uptake suggests that synergistic cross-reaction mechanisms can enhance the uptake of glyoxal, which is a highly important atmospheric species of widespread occurence. To a broader extent, the reaction of carbonyl and hydroxyl groups within atmospheric acidic particles can also occur with other combinations of organic molecules. Whether or not these synergistic cross-reaction mechanisms occur in non-

aqueous particles or organic-dominated particles and to what extent remains to be investigated.

Ultimately, synergistic cross-reaction mechanisms, when present, can significantly influence the gas-particle partitioning of intermediate and semi-volatile organic compounds (I/SVOCs) and thus greatly affect their atmospheric transport and lifetime. ^{18,44} Important physical properties, such as particle optical properties and cloud condensation nucleation activity, can also be greatly altered. ^{48,49,60}

Acknowledgments. This work was funded by the USA National Science Foundation (Grants AGS-1640378 and CHE-1607640).

Supplemental material. The supplemental material includes: Section S5 (tracer ion identification), Section S2 (characteristic timescales of uptake processes), Table S1, Table S2, Table S3, Figure S1, and Figure S2.

Data availability.

Data are available at https://dataverse.harvard.edu/dataverse/SynergisticUptake

References

289

290

291

292

293

294

- (1) Zhang, Y.; Forrister, H.; Liu, J.; Dibb, J.; Anderson, B.; Schwarz, J. P.; Perring, A. E.; Jimenez, J. L.; Campuzano-Jost, P.; Wang, Y.; Nenes, A.; Weber, R. J. Top-of-Atmosphere Radiative Forcing Affected by Brown Carbon in the Upper Troposphere. *Nat. Geosci.* 2017, *10* (7), 486–489. DOI:10.1038/ngeo2960.
- (2) Lelieveld, J.; Pozzer, A.; Po, U.; Fnais, M.; Haines, A.; Mu, T. Loss of Life Expectancy from Air Pollution Compared to Other Risk Factors: Aworldwide Perspective.

 *Cardiovasc. Res. 2020, 3 (1), e26–e39. DOI:10.1093/cvr/cvaa025.
- (3) Chan, C. K.; Yao, X. Air Pollution in Mega Cities in China. Atmos. Environ. 2008, 42 (1),

- 1-42. DOI:10.1016/j.atmosenv.2007.09.003.
- (4) Kanakidou, M.; Seinfeld, J. H.; Pandis, S. N.; Barnes, I.; Dentener, F. J.; Facchini, M. C.; Van Dingenen, R.; Ervens, B.; Nenes, A.; Nielsen, C. J.; Swietlicki, E.; Putaud, J. P.; Balkanski, Y.; Fuzzi, S.; Horth, J.; Moortgat, G. K.; Winterhalter, R.; Myhre, C. E. L.; Tsigaridis, K.; Vignati, E.; Stephanou, E. G.; Wilson, J. Organic Aerosol and Global Climate Modelling: A Review. *Atmos. Chem. Phys.* 2005, *5*, 1053–1123.
 DOI:10.5194/acp-5-1053-2005.
- (5) Kerminen, V. M.; Chen, X.; Vakkari, V.; Petäjä, T.; Kulmala, M.; Bianchi, F. Atmospheric New Particle Formation and Growth: Review of Field Observations. *Environ. Res. Lett.* 2018, *13* (10), 103003. DOI:10.1088/1748-9326/aadf3c.
- (6) Shiraiwa, M.; Yee, L. D.; Schilling, K. a; Loza, C. L.; Craven, J. S.; Zuend, A.; Ziemann, P. J.; Seinfeld, J. H. Size Distribution Dynamics Reveal Particle-Phase Chemistry in Organic Aerosol Formation. *Proc. Natl. Acad. Sci. U. S. A.* 2013, *110* (29), 11746–11750. DOI:10.1073/pnas.1307501110.
- (7) Liu, Y. J.; Kuwata, M.; McKinney, K. A.; Martin, S. T. Uptake and Release of Gaseous Species Accompanying the Reactions of Isoprene Photo-Oxidation Products with Sulfate Particles. *Phys. Chem. Chem. Phys.* 2016, *18* (3), 1595–1600.
 DOI:10.1039/C5CP04551G.
- (8) Riipinen, I.; Yli-Juuti, T.; Pierce, J. R.; Petäjä, T.; Worsnop, D. R.; Kulmala, M.; Donahue, N. M. The Contribution of Organics to Atmospheric Nanoparticle Growth. *Nat. Geosci.* 2012, *5* (7), 453–458. DOI:10.1038/ngeo1499.
- (9) Liu, P.; Song, M.; Zhao, T.; Gunthe, S. S.; Ham, S.; He, Y.; Qin, Y. M.; Gong, Z.; Amorim, J. C.; Bertram, A. K.; Martin, S. T. Resolving the Mechanisms of Hygroscopic

- Growth and Cloud Condensation Nuclei Activity for Organic Particulate Matter. *Nat. Commun.* 2018, *9* (1), 4076. DOI:10.1038/s41467-018-06622-2.
- (10) Gray Bé, A.; Upshur, M. A.; Liu, P.; Martin, S. T.; Geiger, F. M.; Thomson, R. J. Cloud Activation Potentials for Atmospheric α-Pinene and β-Caryophyllene Ozonolysis Products. ACS Cent. Sci. 2017, 3 (7), 715–725. DOI:10.1021/acscentsci.7b00112.
- (11) Kleinman, L. I.; Springston, S. R.; Wang, J.; Daum, P. H.; Lee, Y. N.; Nunnermacker, L. J.; Senum, G. I.; Weinstein-Lloyd, J.; Alexander, M. L.; Hubbe, J.; Ortega, J.; Zaveri, R. A.; Canagaratna, M. R.; Jayne, J. The Time Evolution of Aerosol Size Distribution over the Mexico City Plateau. *Atmos. Chem. Phys.* 2009, 9 (13), 4261–4278. DOI:10.5194/acp-9-4261-2009.
- (12) Goldstein, A. H.; Galbally, I. E. Known and Unexplored Organic Constituents in the Earth's Atmosphere. *Environ. Sci. Technol.* 2007, 41 (5), 1514–1521.
 DOI:10.1021/es072476p.
- (13) Shrivastava, M.; Cappa, C. D.; Fan, J.; Goldstein, A. H.; Guenther, A. B.; Jimenez, J. L.; Kuang, C.; Laskin, A.; Martin, S. T.; Ng, N. L.; Petaja, T.; Pierce, J. R.; Rasch, P. J.; Roldin, P.; Seinfeld, J. H.; Shilling, J.; Smith, J. N.; Thornton, J. A.; Volkamer, R.; Wang, J.; Worsnop, D. R.; Zaveri, R. A.; Zelenyuk, A.; Zhang, Q. Recent Advances in Understanding Secondary Organic Aerosol: Implications for Global Climate Forcing. *Rev. Geophys.* 2017, 55 (2), 509–559. DOI:10.1002/2016RG000540.
- (14) Kolb, C. E.; Cox, R. A.; Abbatt, J. P. D.; Ammann, M.; Davis, E. J.; Donaldson, D. J.;
 Garrett, B. C.; George, C.; Griffiths, P. T.; Hanson, D. R.; Kulmala, M.; McFiggans, G.;
 Pöschl, U.; Riipinen, I.; Rossi, M. J.; Rudich, Y.; Wagner, P. E.; Winkler, P. M.;
 Worsnop, D. R.; O'Dowd, C. D. An Overview of Current Issues in the Uptake of

- Atmospheric Trace Gases by Aerosols and Clouds. *Atmos. Chem. Phys.* 2010, *10* (21), 10561–10605. DOI:10.5194/acp-10-10561-2010.
- (15) Abbatt, J. P. D.; Lee, A. K. Y.; Thornton, J. A. Quantifying Trace Gas Uptake to Tropospheric Aerosol: Recent Advances and Remaining Challenges. *Chem. Soc. Rev.* 2012, 41 (19), 6555–6581. DOI:10.1039/c2cs35052a.
- (16) Seinfeld, J. H.; Pandis, S. N. Atmospheric Chemistry and Physics: From Air Pollution to Climate Change, Third Edition; Wiley: Hoboken, NJ, 2016.
- (17) Kuwata, M.; Liu, Y.; McKinney, K.; Martin, S. T. Physical State and Acidity of Inorganic Sulfate Can Regulate the Production of Secondary Organic Material from Isoprene Photooxidation Products. *Phys. Chem. Chem. Phys.* 2015, *17* (8), 5670–5678.
 DOI:10.1039/c4cp04942j.
- Isaacman-VanWertz, G.; Yee, L. D.; Kreisberg, N. M.; Wernis, R.; Moss, J. A.; Hering, S. V.; De Sá, S. S.; Martin, S. T.; Alexander, M. L.; Palm, B. B.; Hu, W.; Campuzano-Jost, P.; Day, D. A.; Jimenez, J. L.; Riva, M.; Surratt, J. D.; Viegas, J.; Manzi, A.; Edgerton, E.; Baumann, K.; Souza, R.; Artaxo, P.; Goldstein, A. H. Ambient Gas-Particle Partitioning of Tracers for Biogenic Oxidation. *Environ. Sci. Technol.* 2016, 50 (18), 9952–9962.
 DOI:10.1021/acs.est.6b01674.
- (19) Liggio, J.; Li, S. M.; McLaren, R. Heterogeneous Reactions of Glyoxal on Particulate Matter: Identification of Acetals and Sulfate Esters. *Environ. Sci. Technol.* 2005, 39 (6), 1532–1541. DOI:10.1021/es048375y.
- (20) Shiraiwa, M.; Ammann, M.; Koop, T.; Poschl, U. Gas Uptake and Chemical Aging of Semisolid Organic Aerosol Particles. *Proc. Natl. Acad. Sci.* 2011, 108 (27), 11003–11008. DOI:10.1073/pnas.1103045108.

- (21) Kuwata, M.; Martin, S. T. Phase of Atmospheric Secondary Organic Material Affects Its Reactivity. *Proc. Natl. Acad. Sci.* 2012, 109 (43), 17354–17359.
 DOI:10.1073/pnas.1209071109.
- (22) Li, Y. J.; Liu, P.; Gong, Z.; Wang, Y.; Bateman, A. P.; Bergoend, C.; Bertram, A. K.; Martin, S. T. Chemical Reactivity and Liquid/Nonliquid States of Secondary Organic Material. *Environ. Sci. Technol.* 2015, 49 (22), 13264–13274.
 DOI:10.1021/acs.est.5b03392.
- (23) Jang, M.; Kamens, R. M. Atmospheric Secondary Aerosol Formation by Heterogeneous Reactions of Aldehydes in the Presence of a Sulfuric Acid Aerosol Catalyst. *Environ. Sci. Technol.* 2001, *35* (24), 4758–4766. DOI:10.1021/es010790s.
- (24) Kroll, J. H.; Ng, N. L.; Murphy, S. M.; Varutbangkul, V.; Flagan, R. C.; Seinfeld, J. H. Chamber Studies of Secondary Organic Aerosol Growth by Reactive Uptake of Simple Carbonyl Compounds. *J. Geophys. Res. Atmos.* 2005, *110* (23), 1–10. DOI:10.1029/2005JD006004.
- (25) Liggio, J.; Li, S. M. Reactive Uptake of Pinonaldehyde on Acidic Aerosols. *J. Geophys. Res. Atmos.* 2006, *111* (24), 1–12. DOI:10.1029/2005JD006978.
- (26) Gong, Z.; Han, Y.; Liu, P.; Ye, J.; Keutsch, F. N.; McKinney, K. A.; Martin, S. T. Influence of Particle Physical State on the Uptake of Medium-Sized Organic Molecules. *Environ. Sci. Technol.* 2018, *52* (15), 8381–8389. DOI:10.1021/acs.est.8b02119.
- (27) Han, Y.; Gong, Z.; Ye, J.; Liu, P.; McKinney, K. A.; Martin, S. T. Quantifying the Role of the Relative Humidity-Dependent Physical State of Organic Particulate Matter in the Uptake of Semivolatile Organic Molecules. *Environ. Sci. Technol.* 2019, 53 (22), 13209– 13218. DOI:10.1021/acs.est.9b05354.

- (28) Liu, P.; Li, Y. J.; Wang, Y.; Bateman, A. P.; Zhang, Y.; Gong, Z.; Bertram, A. K.; Martin, S. T. Highly Viscous States Affect the Browning of Atmospheric Organic Particulate Matter. ACS Cent. Sci. 2018, 4 (2), 207–215. DOI:10.1021/acscentsci.7b00452.
- (29) Fu, T. M.; Jacob, D. J.; Wittrock, F.; Burrows, J. P.; Vrekoussis, M.; Henze, D. K. Global Budgets of Atmospheric Glyoxal and Methylglyoxal, and Implications for Formation of Secondary Organic Aerosols. *J. Geophys. Res. Atmos.* 2008, *113* (D15), D15303. DOI:10.1029/2007JD009505.
- (30) Liggio, J.; Li, S. M.; McLaren, R. Reactive Uptake of Glyoxal by Particulate Matter. *J. Geophys. Res. D Atmos.* 2005, *110* (10), 1–13. DOI:10.1029/2004JD005113.
- (31) Curry, L. A.; Tsui, W. G.; McNeill, V. F. Technical Note: Updated Parameterization of the Reactive Uptake of Glyoxal and Methylglyoxal by Atmospheric Aerosols and Cloud Droplets. *Atmos. Chem. Phys.* 2018, *18* (13), 9823–9830. DOI:10.5194/acp-18-9823-2018.
- (32) Ervens, B.; Volkamer, R. Glyoxal Processing by Aerosol Multiphase Chemistry: Towards a Kinetic Modeling Framework of Secondary Organic Aerosol Formation in Aqueous Particles. *Atmos. Chem. Phys.* 2010, *10* (17), 8219–8244. DOI:10.5194/acp-10-8219-2010.
- (33) Whipple, E. B. The Structure of Glyoxal in Water. *J. Am. Chem. Soc.* 1970, *92*, 7183–7186. DOI:10.1021/ja00727a027.
- (34) Hastings, W. P.; Koehler, C. A.; Bailey, E. L.; De Haan, D. O. Secondary Organic Aerosol Formation by Glyoxal Hydration and Oligomer Formation: Humidity Effects and Equilibrium Shifts during Analysis. *Environ. Sci. Technol.* 2005, *39*, 8728–8735. DOI:10.1021/es0504461.

- Loza, C. L.; Chan, A. W. H.; Galloway, M. M.; Keutsch, F. N.; Flagan, R. C.; Seinfeld, J. H. Characterization of Vapor Wall Loss in Laboratory Chambers. *Environ. Sci. Technol.*2010, 44 (13), 5074–5078. DOI:10.1021/es100727v.
- (36) Decarlo, P. F.; Kimmel, J. R.; Trimborn, A.; Northway, M. J.; Jayne, J. T.; Aiken, A. C.; Gonin, M.; Fuhrer, K.; Horvath, T.; Docherty, K. S.; Worsnop, D. R.; Jimenez, J. L. Field-Deployable, High-Resolution, Time-of-Flight Aerosol Mass Spectrometer. *Anal. Chem.* 2006, 78 (24), 8281–8289. DOI:8410.1029/2001JD001213. Analytical.
- (37) Galloway, M. M.; Chhabra, P. S.; Chan, A. W. H.; Surratt, J. D.; Flagan, R. C.; Seinfeld, J. H.; Keutsch, F. N. Glyoxal Uptake on Ammonium Sulphate Seed Aerosol: Reaction Products and Reversibility of Uptake under Dark and Irradiated Conditions. *Atmos. Chem. Phys.* 2009, 9 (10), 3331–3345. DOI:org/10.5194/acp-9-3331-2009.
- (38) Volkamer, R.; Ziemann, P. J.; Molina, M. J. Secondary Organic Aerosol Formation from Acetylene (C2H2): Seed Effect on SOA Yields Due to Organic Photochemistry in the Aerosol Aqueous Phase. *Atmos. Chem. Phys.* 2009, *9* (6), 1907–1928. DOI:10.5194/acp-9-1907-2009.
- (39) Healy, R. M.; Temime, B.; Kuprovskyte, K.; Wenger, J. C. Effect of Relative Humidity on Gas/Particle Partitioning and Aerosol Mass Yield in the Photooxidation of p-Xylene.

 Environ. Sci. Technol. 2009, 43 (6), 1884–1889. DOI:10.1021/es802404z.
- (40) Shen, H.; Chen, Z.; Li, H.; Qian, X.; Qin, X.; Shi, W. Gas-Particle Partitioning of Carbonyl Compounds in the Ambient Atmosphere. *Environ. Sci. Technol.* 2018, *52* (19), 10997–11006. DOI:10.1021/acs.est.8b01882.
- (41) Jang, M.; Czoschke, N. M.; Northcross, A. L. Atmospheric Organic Aerosol Production by Heterogeneous Acid-Catalyzed Reactions. *ChemPhysChem* 2004, *5* (11), 1646–1661.

- DOI:10.1002/cphc.200301077.
- (42) Clegg, S. L.; Seinfeld, J. H.; Edney, E. O. Thermodynamic Modelling of Aqueous Aerosols Containing Electrolytes and Dissolved Organic Compounds. II. An Extended Zdanovskii-Stokes-Robinson Approach. *J. Aerosol Sci.* 2003, 34 (6), 667–690. DOI:10.1016/S0021-8502(03)00019-3.
- (43) Jang, M.; Czoschke, N. M.; Lee, S.; Kamens, R. M. Heterogeneous Atmospheric Aerosol Production by Acid-Catalyzed Particle-Phase Reactions. *Science* (80-.). 2002, 298 (5594), 814–817. DOI:10.1126/science.1075798.
- (44) Shen, H.; Chen, Z.; Li, H.; Qian, X.; Qin, X.; Shi, W. Gas-Particle Partitioning of Carbonyl Compounds in the Ambient Atmosphere. *Environ. Sci. Technol.* 2018, *52* (19), 10997–11006. DOI:10.1021/acs.est.8b01882.
- (45) Minerath, E. C.; Casale, M. T.; Elrod, M. J. Kinetics Feasibility Study of Alcohol Sulfate Esterification Reactions in Tropospheric Aerosols. *Environ. Sci. Technol.* 2008, 42 (12), 4410–4415. DOI:10.1021/es8004333.
- (46) Chan, L. P.; Lee, A. K. Y.; Chan, C. K. Gas-Particle Partitioning of Alcohol Vapors on Organic Aerosols. *Environ. Sci. Technol.* 2010, 44 (1), 257–262. DOI:10.1021/es9018018.
- (47) Hamilton, J. F.; Baeza-Romero, M. T.; Finessi, E.; Rickard, A. R.; Healy, R. M.; Peppe, S.; Adams, T. J.; Daniels, M. J. S.; Ball, S. M.; Goodall, I. C. A.; Monks, P. S.; Borrás, E.; Muñoz, A. Online and Offline Mass Spectrometric Study of the Impact of Oxidation and Ageing on Glyoxal Chemistry and Uptake onto Ammonium Sulfate Aerosols. *Faraday Discuss.* 2013, 165, 447–472. DOI:10.1039/c3fd00051f.
- (48) Yu, G.; Bayer, A. R.; Galloway, M. M.; Korshavn, K. J.; Fry, C. G.; Keutsch, F. N. Glyoxal in Aqueous Ammonium Sulfate Solutions: Products, Kinetics and Hydration

- Effects. Environ. Sci. Technol. 2011, 45 (15), 6336-6342. DOI:10.1021/es200989n.
- (49) Gen, M.; Huang, D.; Chan, C. K. Reactive Uptake of Glyoxal by Ammonium Containing Salt Particles as a Function of Relative Humidity. *Environ. Sci. Technol.* 2018, *52*, 6903–6911. DOI:10.1021/acs.est.8b00606.
- (50) Barsanti, K. C.; Pankow, J. F. Thermodynamics of the Formation of Atmospheric Organic Particulate Matter by Accretion Reactions 2. Dialdehydes, Methylglyoxal, and Diketones. *Atmos. Environ.* 2005, *39* (35), 6597–6607.

 DOI:10.1016/j.atmosenv.2005.07.056.
- (51) Loeffler, K. W.; Koehler, C. A.; Paul, N. M.; De Haan, D. O. Oligomer Formation in Evaporating Aqueous Glyoxal and Methyl Glyoxal Solutions. *Environ. Sci. Technol.* 2006, 40 (20), 6318–6323. DOI:10.1021/es060810w.
- (52) Corrigan, A. L.; Hanley, S. W.; De Haan, D. O. Uptake of Glyoxal by Organic and Inorganic Aerosol. *Environ. Sci. Technol.* 2008, 42 (12), 4428–4433.
 DOI:10.1021/es7032394.
- (53) Drozd, G. T.; McNeill, V. F. Organic Matrix Effects on the Formation of Light-Absorbing Compounds from α-Dicarbonyls in Aqueous Salt Solution. *Environ. Sci. Process. Impacts* 2014, *16* (4), 741–747. DOI:10.1039/c3em00579h.
- (54) De Haan, D. O.; Corrigan, A. L.; Tolbert, M. A.; Jimenez, J. L.; Wood, S. E.; Turley, J. J. Secondary Organic Aerosol Formation by Self-Reactions of Methylglyoxal and Glyoxal in Evaporating Droplets. *Environ. Sci. Technol.* 2009, 43 (21), 8184–8190.
 DOI:10.1021/es902152t.
- (55) Faust, J. A.; Wong, J. P. S.; Lee, A. K. Y.; Abbatt, J. P. D. Role of Aerosol Liquid Water in Secondary Organic Aerosol Formation from Volatile Organic Compounds. *Environ*.

- Sci. Technol. 2017, 51 (3), 1405–1413. DOI:10.1021/acs.est.6b04700.
- (56) Riva, M.; Heikkinen, L.; Bell, D. M.; Peräkylä, O.; Zha, Q.; Schallhart, S.; Rissanen, M. P.; Imre, D.; Petäjä, T.; Thornton, J. A.; Zelenyuk, A.; Ehn, M. Chemical Transformations in Monoterpene-Derived Organic Aerosol Enhanced by Inorganic Composition. *npj Clim. Atmos. Sci.* 2019, 2 (1). DOI:10.1038/s41612-018-0058-0.
- (57) Pöschl, U.; Rudich, Y.; Ammann, M. Kinetic Model Framework for Aerosol and Cloud Surface Chemistry and Gas-Particle Interactions - Part 1: General Equations, Parameters, and Terminology. *Atmos. Chem. Phys.* 2007, 7 (23), 5989–6023. DOI:10.5194/acp-7-5989-2007.
- (58) Ditto, J. C.; Joo, T.; Slade, J. H.; Shepson, P. B.; Ng, N. L.; Gentner, D. R. Nontargeted Tandem Mass Spectrometry Analysis Reveals Diversity and Variability in Aerosol Functional Groups across Multiple Sites, Seasons, and Times of Day. *Environ. Sci. Technol. Lett.* 2020, 7 (2), 60–69. DOI:10.1021/acs.estlett.9b00702.
- (59) Russell, L. M.; Bahadur, R.; Ziemann, P. J. Identifying Organic Aerosol Sources by Comparing Functional Group Composition in Chamber and Atmospheric Particles. *Proc. Natl. Acad. Sci. U. S. A.* 2011, *108* (9), 3516–3521. DOI:10.1073/pnas.1006461108.
- (60) Sareen, N.; Schwier, A. N.; Lathem, T. L.; Nenes, A.; McNeill, V. F. Surfactants from the Gas Phase May Promote Cloud Droplet Formation. *Proc. Natl. Acad. Sci. U. S. A.* 2013, 110 (8), 2723–2728. DOI:10.1073/pnas.1204838110.

List of Figures

- **Figure 1.** A schematic diagram of the experimental setup. Abbreviations: AMS, high-resolution time-of-flight aerosol mass spectrometer; SMPS, scanning mobility particle sizer.
- **Figure 2.** Time series plots demonstrating glyoxal and pinanediol uptake by (I) acidic sulfate particles and (II) neutral sulfate particles. (a) Uptake of glyoxal. (b) Uptake of pinanediol. (c) Uptake for a mixture of glyoxal and pinanediol at the same concentrations as panels a and b. Table S1 lists the gas-phase concentrations. Other conditions: ammonium bisulfate particle concentration, $37 \pm 2 \mu g m^{-3}$; ammonium sulfate particle concentration, $75 \pm 5 \mu g m^{-3}$.
- Figure 3. Dependence of uptake on relative humidity. (a) Glyoxal uptake by ammonium bisulfate particles for blank (i.e., absence of organic gas-phase species), unary glyoxal, and binary mixture of glyoxal and pinanediol. (b) Pinanediol uptake by ammonium bisulfate particles for blank, unary pinanediol, and binary mixture of glyoxal and pinanediol. The gas-phase concentrations are the same as in Figure 2. No experiment was conducted at 10% RH for unary pinanediol because of experimental difficulties.
- **Figure 4.** Proposed reaction mechanisms of synergistic glyoxal and pinanediol uptake by ammonium bisulfate particles.
- **Figure 5.** AMS organic mass spectra observed using (a) uptake of glyoxal, (b) uptake of pinanediol, and (c) uptake of a mixture of glyoxal and pinanediol to ammonium bisulfate particles. The gas-phase concentrations are the same as in Figure 2.

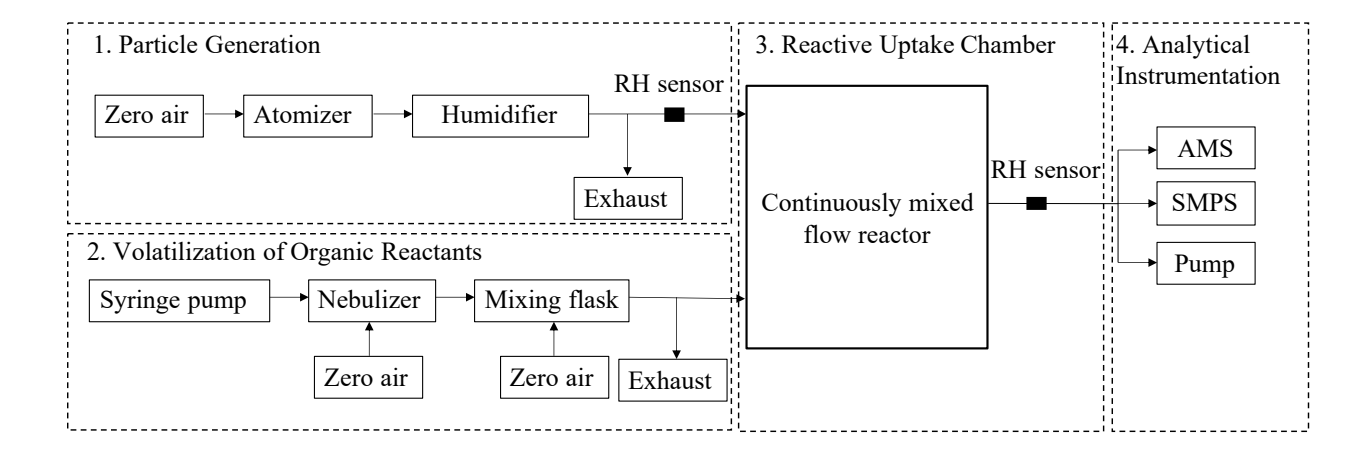


Figure 1

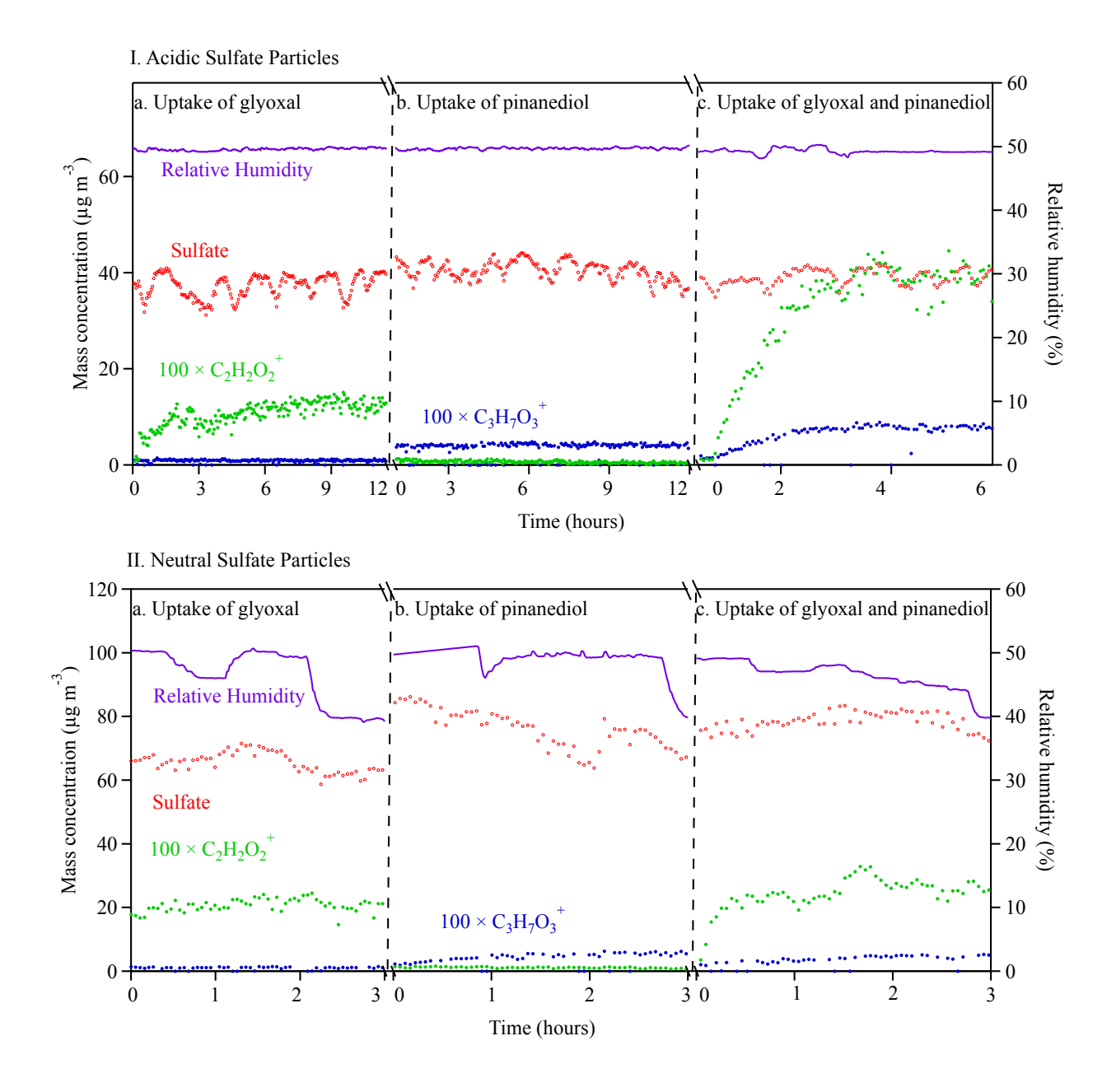


Figure 2

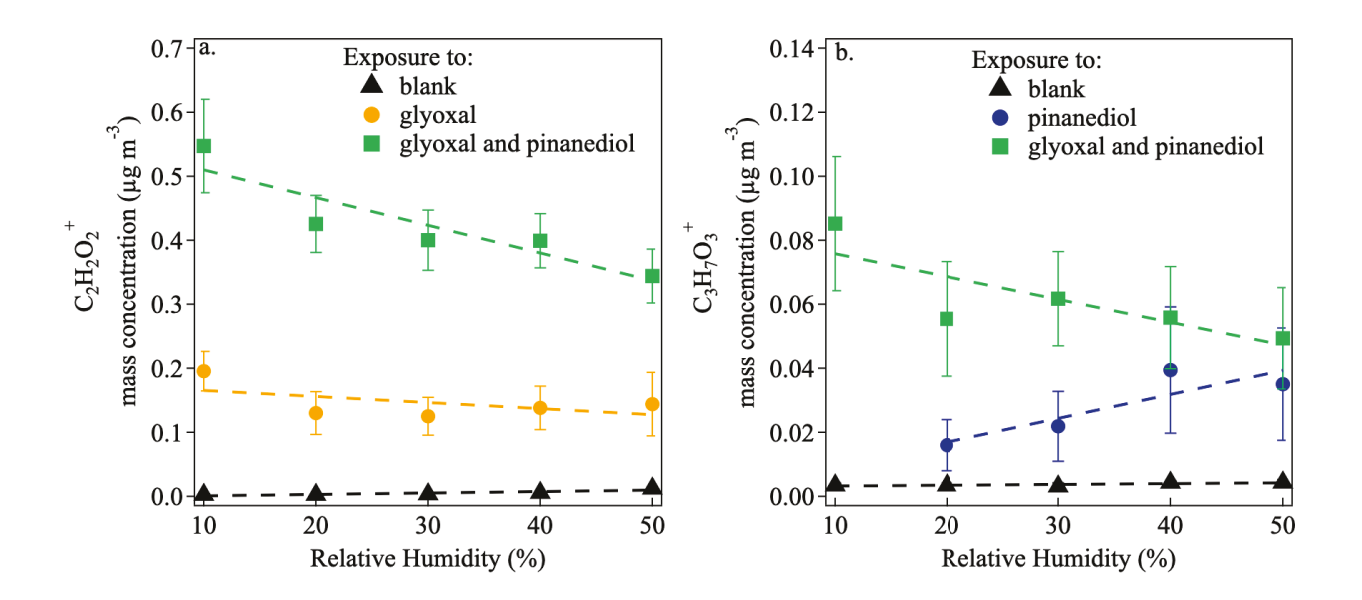


Figure 3

Figure 4

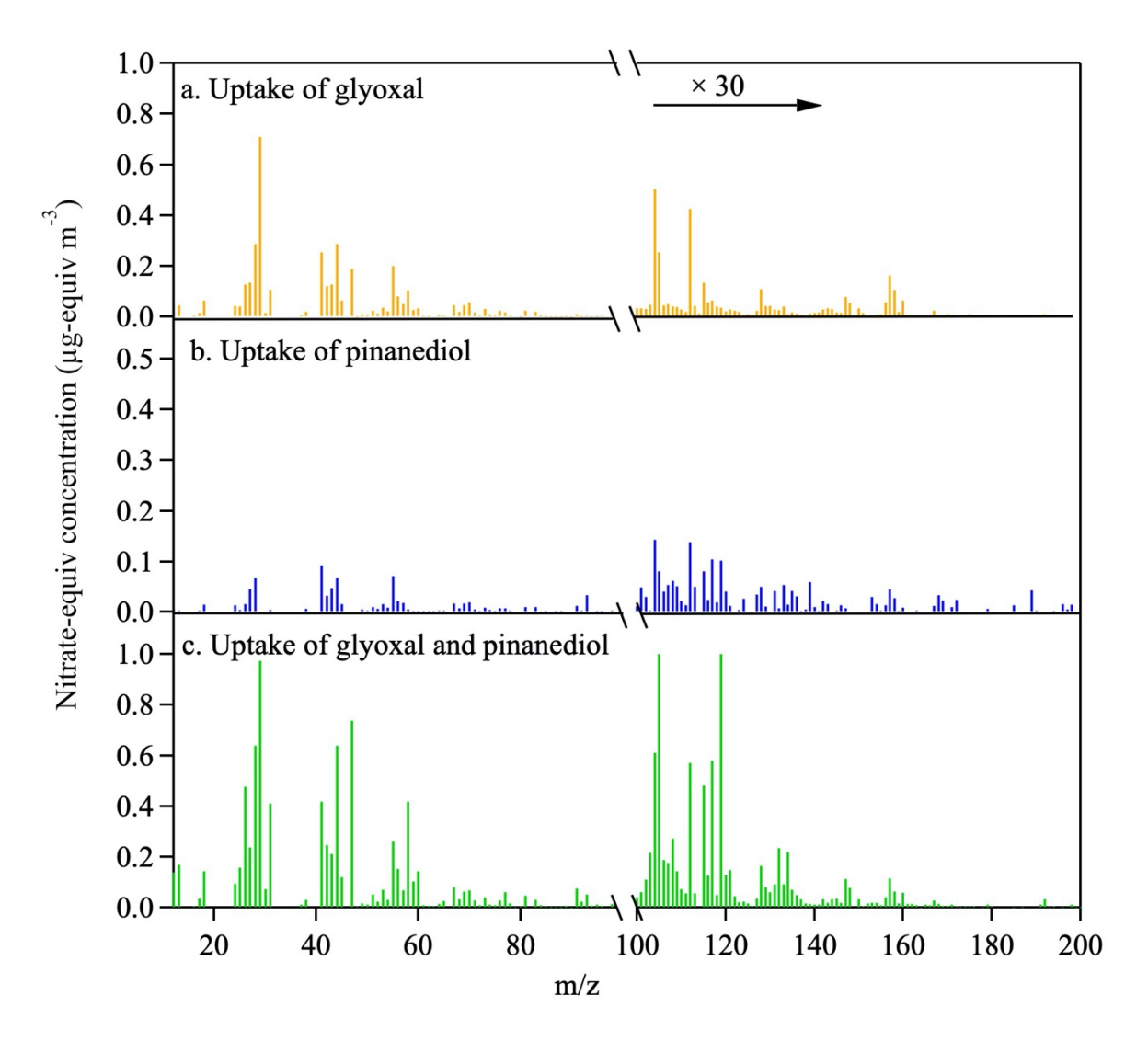


Figure 5

Supplemental Material

Synergistic Uptake by Acidic Sulfate Particles of Gaseous Mixtures of Glyoxal and Pinanediol

Yiming Qin (1), Jianhuai Ye (1), Paul E. Ohno (1,2), Yali Lei (1), Junfeng Wang (1), Pengfei Liu (1), Regan J. Thomson (3), and Scot T. Martin* (1,4)

- School of Engineering and Applied Sciences, Harvard University, Cambridge, Massachusetts, USA
- (2) Harvard University Center for the Environment, Harvard University, Cambridge,
 Massachusetts, USA
- (3) Department of Chemistry, Northwestern University, Evanston, Illinois, USA
- (4) Department of Earth and Planetary Sciences, Harvard University, Cambridge, Massachusetts, USA

E-mail: scot martin@harvard.edu, ORCiD: 0000-0002-8996-7554

http://martin.seas.harvard.edu

Supplemental material

- 2 The supplemental material includes: Section S6 (tracer ion identification), Section S2
- 3 (characteristic timescales of uptake processes), Table S1, Table S2, Table S3, Figure S1, and
- 4 Figure S2.

1

5

6

7

8

9

10

11

12

13

14

15

16

17

18

19

20

21

S7. Tracer ion identification

Figure S1 shows the signal intensity for aerosol particles sampled by the AMS at m/z 58 and m/z 91, identified here as tracer ions for glyoxal and pinanediol, respectively. The blank condition (black circles) corresponds to the injection of ammonium bisulfate particles to the CMFR in the absence of any organic gas-phase species. For this condition, there is no appreciable intensity at either m/z ratio, indicating no contribution at these m/z ratios by any other species in the absence of glyoxal and pinanediol. For the unary uptake of glyoxal (orange circles; gas-phase mixing ratio 58 ppb) by ammonium bisulfate particles, a large increase in the signal intensity at m/z 58 (C₂H₂O₂⁺) is seen as compared to the blank condition. The same tracer ion has previously been used in the literature to track glyoxal uptake. No contribution at m/z 91 was observed for these glyoxal-only experiments. For the unary uptake of pinanediol (blue circles; gas-phase mixing ratio 20 ppb) by ammonium bisulfate particles, a peak is observed at m/z 91, while no contribution at m/z 58 was observed. For the binary uptake of glyoxal and pinanediol (green circles; same gas-phase mixing ratios as their unary counterparts), appreciable signal intensity is seen at both m/z 58 and m/z 91, as expected. Notably, the signal intensities at both m/z 58 and m/z 91 increase in the binary mixture system, as compared to their unary counterparts, by factors of 3.7 and 2.3, respectively.

S8. Characteristic timescales of uptake processes

As described in the main text, the extent of uptake observed under a certain set of laboratory conditions might be limited be either kinetic or thermodynamic factors. The uptake of gaseous species to the particle phase can be considered within the framework of five sequential steps: (i) diffusion of a molecule in the gas phase to the gas-particle interface, (ii) accommodation of the molecule into the particle surface region, (iii) possible chemical reactions within the surface region, (iv) diffusion of the molecule from the surface to the interior region of the particle phase, and (v) possible chemical reactions within the interior region of the particle phase.³ The characteristic timescale of the whole process is set by the limiting step.^{4,5} **Step i.**

The characteristic timescale τ_g for gas-phase diffusion is formulated as follows:³

$$\tau_{g} = \frac{R_{p}^{2}}{4D_{g}} \tag{1}$$

where R_p is the particle radius and D_g is gas diffusivity. At 25 °C and 1 atm, D_g is 1.9×10^{-5} m² s⁻¹. For polydisperse particles in a typical experiment, where R_p ranges from 30 nm to 200 nm, τ_g ranges from 2.9×10^{-12} to 1.3×10^{-10} s, which is much less than $\tau_{\rm exp}$ of 390 s. Thus, gas-phase diffusion is effectively instantaneous compared to the experimental exposure timescale and is not the limiting factor in the uptake process.

39 Step ii.

The characteristic timescale to achieve equilibrium at the gas-particle interface for soluble gases can be approximated as follows:³

$$\tau_{g-p} = \frac{R_p K_H \sqrt{2\pi M_W RT}}{3\alpha} \tag{2}$$

where K_H is the effective Henry's law constant (mol L⁻¹atm⁻¹), M_W is molecular weight of the gas molecules (g mol⁻¹), and α is the accommodation coefficient. The accommodation coefficient typically ranges from 0.1 to 1.³ Depending on the solvent and its concentration, K_H for glyoxal ranges from 3.6×10^5 to 2.3×10^8 mol L⁻¹ atm⁻¹ while K_H for pinanediol ranges from 4.1×10^3 to 5.2×10^7 mol L⁻¹ atm⁻¹.⁶ Therefore, the characteristic timescale for accommodation of these species at the surface of the particles is in the range of 5×10^{-4} to 22 s for glyoxal and 1×10^{-5} to 9 s for pinanediol. These estimates indicate that Henry's law equilibrium is established at the interface during the experimental timescale of 390 s.

51 Step iii.

The characteristic timescale of diffusion within the particle phase can be estimated based on the size and the diffusivity of the particle, as follows:³

$$\tau_{p} = \frac{R_{p}^{2}}{\pi D_{p}} \tag{3}$$

where D_p is the particle diffusivity. The generation of ammonium bisulfate and ammonium sulfate particles by atomization of an aqueous solution results in initially liquid-phase particles. At 25 °C and 1 atm, the efflorescence RH of ammonium sulfate is in the range of 28% - 42% RH while ammonium bisulfate typically does not effloresce. Therefore, in the experimental conditions of this study (ammonium sulfate particles at 50% RH and ammonium bisulfate particles at RH ranging from 10%-50%), the particles remain in the liquid phase. The diffusivity of small molecules in concentrated salt particles is 1×10^{-10} m² s⁻¹ (e.g., 100% sulfuric acid)⁸ and the corresponding τ_p is less than 2.5×10^{-5} s, indicating that particle-phase diffusion is not a kinetic limitation during the experimental timescale.

Step iv.

The fast diffusion of the dissolved organic species calculated above indicates rapid mixing throughout the particle, and thus no significant concentration gradient develops inside the particle. Therefore, the localized surface reactions and aqueous bulk phase reactions are not distinguished in the estimate of chemical reactions herein. In a case for which Henry's law equilibrium is established and the reactants diffuse throughout the particle, the characteristic timescale of chemical reaction can be estimated based on the reaction rates of those proposed in the main text. In the case of unary glyoxal uptake, the characteristic timescale is the inverse of the reaction rate k of glyoxal with the ions in the initially organic-free sulfate particles. In the case of synergistic uptake, the characteristic reaction timescale of each species can be estimated by a second-order chemical reaction, as follows:

$$\tau_{rxn} = \frac{1}{kK_{H}P_{r}} \tag{4}$$

where k is the rate coefficient for the reaction and P_x is the partial pressure of the other reacting species. The product $K_H P_x$ equals the concentration of the other species in the particle phase. A complication is that the specific rates of reactions proposed in this study are not known.

Reactions of carbonyls and alcohols forming hemiacetals in bulk solution reach equilibrium at a time scale of 1 to 10 h depending on the acidity. These timescales are longer than the residence time of 390s in the CMFR. Particle-phase reactions, however, can be much faster than those in the bulk solution due to the high ionic concentrations reached inside particles. Further investigation is required to examine the reaction rate between glyoxal and alcohols in the particle phase. Slow aqueous-phase chemical reactions may not reach equilibrium during the experimental CMFR residence time of 390 s, implying in this case that the observed uptake could be in a kinetically limited regime. Similar uptake (i.e., in the thermodynamic region) or

- greater uptake (i.e., in the kinetic regime) compared to the laboratory experiments is thus
- 88 expected for the longer interaction times of atmospheric processes.

References

- (1) Galloway, M. M.; Chhabra, P. S.; Chan, A. W. H.; Surratt, J. D.; Flagan, R. C.; Seinfeld, J. H.; Keutsch, F. N. Glyoxal Uptake on Ammonium Sulphate Seed Aerosol: Reaction Products and Reversibility of Uptake under Dark and Irradiated Conditions. *Atmos. Chem. Phys.* 2009, 9 (10), 3331–3345. DOI:org/10.5194/acp-9-3331-2009.
- (2) Clegg, S. L.; Seinfeld, J. H.; Edney, E. O. Thermodynamic Modelling of Aqueous Aerosols Containing Electrolytes and Dissolved Organic Compounds. II. An Extended Zdanovskii-Stokes-Robinson Approach. *J. Aerosol Sci.* 2003, 34 (6), 667–690. DOI:10.1016/S0021-8502(03)00019-3.
- (3) Seinfeld, J. H.; Pandis, S. N. Atmospheric Chemistry and Physics: From Air Pollution to Climate Change, Third Edition; 2016. Wiley: Hoboken, NJ, 2016.
- (4) Ervens, B.; Volkamer, R. Glyoxal Processing by Aerosol Multiphase Chemistry: Towards a Kinetic Modeling Framework of Secondary Organic Aerosol Formation in Aqueous Particles. *Atmos. Chem. Phys.* 2010, *10* (17), 8219–8244. DOI:10.5194/acp-10-8219-2010.
- (5) Pöschl, U.; Rudich, Y.; Ammann, M. Kinetic Model Framework for Aerosol and Cloud Surface Chemistry and Gas-Particle Interactions - Part 1: General Equations, Parameters, and Terminology. *Atmos. Chem. Phys.* 2007, 7 (23), 5989–6023. DOI:10.5194/acp-7-5989-2007.
- Kampf, C. J.; Waxman, E. M.; Slowik, J. G.; Dommen, J.; Pfaffenberger, L.; Praplan, A.
 P.; Prévoît, A. S. H.; Baltensperger, U.; Hoffmann, T.; Volkamer, R.; Pfa, L.; Praplan, A.
 P.; Pre, A. S. H.; Baltensperger, U.; Ho, T.; Volkamer, R. Effective Henry's Law
 Partitioning and the Salting Constant of Glyoxal in Aerosols Containing Sulfate. *Environ*.

- Sci. Technol. 2013, 47 (9), 4236-4244. DOI:10.1021/es400083d.
- (7) Martin, S. T. Phase Transitions of Aqueous Atmospheric Particles. *Chem. Rev.* 2000, *100*(9), 3403–3453. DOI:10.1021/cr990034t.
- (8) Rhodes, F. H.; Barbour, C. B. The Viscosities of Mixtures of Sulfuric Acid and Water. Ind. Eng. Chem. 1923, 15 (8), 850–852. DOI:10.1021/ie50164a033.
- (9) Ziemann, P. J.; Atkinson, R. Kinetics, Products, and Mechanisms of Secondary Organic Aerosol Formation. *Chem. Soc. Rev.* 2012, *41* (19), 6582–6605. DOI:10.1039/c2cs35122f.

Table S1. Gas-phase-equivalent injected concentrations of glyoxal and pinanediol in the unary and binary systems. Section 2.3 explains that the injected concentrations are upper limits because of possible wall loss; however, the relative concentrations in unary and binary experiments are expected to be the same because of similar experimental protocols and identical physical apparatus.

Gas-phase species	Unary glyoxal (ppbv)	Unary pinanediol (ppbv)	Binary glyoxal and pinanediol (ppbv)		
Glyoxal	58	N/A	58		
Pinanediol	N/A	20	28		

Table S2. Effect of acidity on the mass-normalized uptake of glyoxal and pinanediol tracers (C₂H₂O₂⁺ and C₃H₇O₃⁺, respectively) by sulfate particles in the unary and binary glyoxal and pinanediol systems. Particle-phase water and pH are estimated using *Extended AIM Aerosol Thermodynamics Model II.*² *Neutral particles. **Acidic particles.

Seed Particle	Gas-Phase Organic Molecules	Sulfate (µg m ⁻³)	Ammonium (μg m ⁻³)	Organic tracer (μg m ⁻³)	Water (µg m ⁻³)	рН	Organic tracer : Sulfate	Organic tracer : (Sulfate + Ammonium)	Organic tracer : (Sulfate + Ammonium + Water)
Ammonium Sulfate*	Unary Glyoxal	69.4	25.9	0.2	44.3	2.2	0.0029	0.0021	0.0014
Ammonium Sulfate	Binary Glyoxal	77.7	29.1	0.24	49.6	2.6	0.0031	0.0022	0.0015
Ammonium Bisulfate**	Unary Glyoxal	35.7	6.8	0.14	19.6	-1.5	0.0039	0.0033	0.0023
Ammonium Bisulfate	Binary Glyoxal	36.6	6.8	0.34	20.8	-1.6	0.0093	0.0078	0.0053
Ammonium Sulfate	Unary Pinanediol	78.2	29	0.053	49.9	2.37	0.00068	0.00049	0.00034
Ammonium Sulfate	Binary Pinanediol	77.7	29	0.049	49.58	2.62	0.00063	0.00046	0.00031
Ammonium Bisulfate	Unary Pinanediol	38.5	8	0.035	19.29	-1.43	0.00091	0.00076	0.00053
Ammonium Bisulfate	Binary Pinanediol	36.6	7	0.049	20.8	-1.57	0.00134	0.00113	0.00076

Table S3. Effect of relative humidity on the mass-normalized uptake of glyoxal and pinanediol tracers $(C_2H_2O_2^+ \text{ and } C_3H_7O_3^+,$ respectively) by acidic sulfate particles in the unary and binary glyoxal and pinanediol systems. Particle-phase water and pH are estimated using *Extended AIM Aerosol Thermodynamics Model II*.²

RH (%)	Gas-Phase Organic Molecules	Sulfate (µg m ⁻³)	Ammoniu m (μg m ⁻³)	Organic tracer (μg m ⁻³)	Water (μg m ⁻³)	pН	Organic tracer : Sulfate	Organic tracer : (Sulfate + Ammonium)	Organic tracer : (Sulfate + Ammonium + Water)
50	Unary Glyoxal	35.7	6.785	0.14 ± 0.05	19.62	-1.5	0.0039	0.0033	0.0023
50	Binary Glyoxal	36.6	6.785	0.34 ± 0.04	20.80	-1.6	0.0093	0.0078	0.0053
40	Unary Glyoxal	35.8	6.555	0.13 ± 0.03 ,	13.92	-2.0	0.0036	0.0031	0.0023
40	Binary Glyoxal	36.5	6.555	0.39 ± 0.04	14.70	-2.0	0.0107	0.0091	0.0068
30	Unary Glyoxal	36.3	7.015	0.12 ± 0.03	7.29	-2.5	0.0033	0.0028	0.0024
30	Binary Glyoxal	37.6	7.13	0.4 ± 0.05	8.01	-2.5	0.0106	0.0089	0.0076
20	Unary Glyoxal	35.3	6.785	0.13 ± 0.03	3.19	-2.9	0.0037	0.0031	0.0029
20	Binary Glyoxal	36.6	6.9	0.43 ± 0.04	3.58	-3.0	0.0117	0.0099	0.0091
10	Unary Glyoxal	33.9	6.44	0.19 ± 0.03	0.99	-3.3	0.0056	0.0047	0.0046
10	Binary Glyoxal	36.5	7.36	0.55 ± 0.07	0.90	-3.0	0.0151	0.0125	0.0123
50	Unary Pinanediol	38.5	7.82	0.035 ± 0.017	19.29	-1.4	0.0009	0.0008	0.0005

50	Binary Pinanediol	36.6	6.785	0.049 ± 0.016	20.80	-1.6	0.0013	0.0011	0.0008
40	Unary Pinanediol	41.7	8.165	0.039 ± 0.019	14.18	-1.9	0.0009	0.0008	0.0006
40	Binary Pinanediol	36.5	6.555	0.056 ± 0.016	14.70	-2.0	0.0015	0.0013	0.0010
30	Unary Pinanediol	33.8	6.555	0.022 ± 0.011	6.71	-2.4	0.0007	0.0005	0.0005
30	Binary Pinanediol	37.6	7.13	0.062 ± 0.015	8.01	-2.5	0.0016	0.0014	0.0012
20	Unary Pinanediol	36.7	7.245	0.016 ± 0.008	2.98	-2.8	0.0004	0.0004	0.0003
20	Binary Pinanediol	36.6	6.9	0.055 ± 0.002	3.58	-3.0	0.0015	0.0013	0.0012
10	Binary Pinanediol	36.5	7.36	0.085 ± 0.021	0.90	-3.0	0.0023	0.0019	0.0019

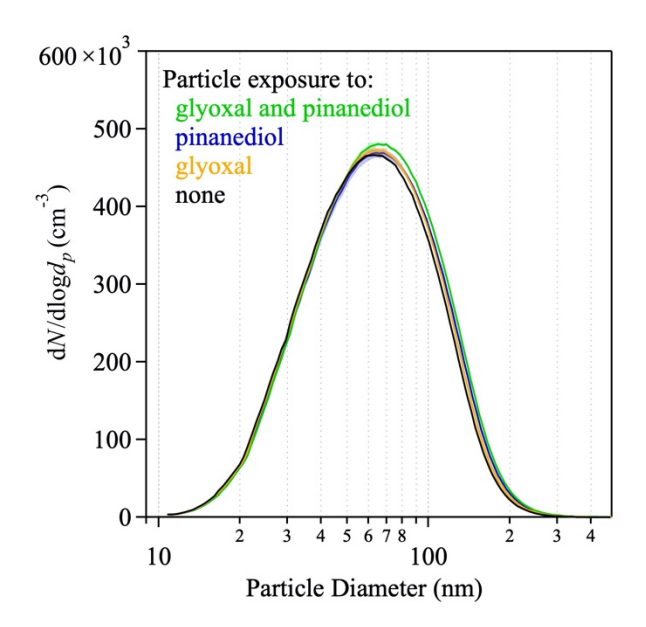


Figure S6. Particle number-diameter distributions for the uptake of glyoxal and pinanediol by ammonium bisulfate particles at 50% RH.

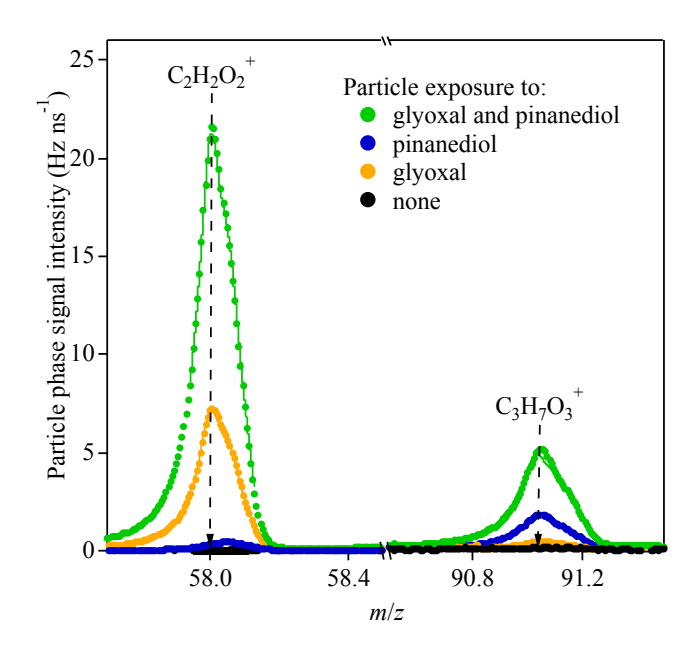


Figure S7. Particle-phase tracer ions for the uptake of glyoxal and pinanediol by ammonium bisulfate particles at 50% RH and 20 °C. The $C_2H_2O_2^+$ and $C_3H_7O_3^+$ ions are tracers of glyoxal and pinanediol respectively.